Investigation of bidirectional three-phase four-leg converter with LCL filter

Nikita A. Dobroskok, Anastasiia D. Stotckaia, Ruslan M. Migranov, Victor S. Lavrinovskiy, Perevalov Yurii Yurievich, Artem S. Melnikov, Vyacheslav Parmenov, Nazar V. Maslennikov
Department of Automatic Control Systems, Faculty of Industrial Automation and Electrical Engineering,
Saint Petersburg Electrotechnical University "LETI", Saint Petersburg, Russia

Article Info

ABSTRACT

A three-phase four-leg bidirectional power converter used as an input stage of an energy storage system using the inductance (L), capacitance (C), and inductance (L) or LCL filter on the grid side is considered. The article provides a variant of the three-phase four-leg bidirectional converter control system implementation based on 3D space vector pulse-width modulation and per-phase voltage control. A brief analysis of the applied control algorithms of the three-phase four-leg bidirectional converter in inverter and rectifier modes is given. A computer model has been built to investigate the operating modes of the converters of the designated class with both balanced and unbalanced load. Studies were carried out by computer modeling methods in order to optimize the parameters of the LCL filter on the grid side with bidirectional energy exchange. Optimal LCL filter parameters and modulation frequencies are determined for the developed converter, providing acceptable quality indicators when operating in bidirectional mode.

Corresponding Author:

Nikita A. Dobroskok
Department of Automatic Control Systems, Faculty of Industrial Automation and Electrical Engineering
Saint Petersburg Electrotechnical University "LETI"
Ulitsa Professora Popova 5, 197022 Saint Petersburg, Russia
Email: nadobroskok@etu.ru

1. INTRODUCTION

At present, there is an active development of alternative energy based on photovoltaic plants, and wind generators, as part of microgrid or distributed generation grids [1]–[4]. Studies [5], [6] show that for the sustainable operation of microgrid based on renewable energy sources, where energy storage system must be a necessary element of the control system, which according to [5] solves at least the following main functions: i) Increasing the limits of static and dynamic stability by compensating for sudden voltage drops caused by the use of renewable energy sources; ii) Suppression of fluctuations in the active and reactive components of load power; and iii) Ensuring of uninterrupted power supply (UPS) to own needs and especially essential consumers. Comparative analysis of batteries is a separate direction of modern research [7]–[10], as well as structures of energy storage systems and energy exchange control systems [11]–[13].

This paper discusses an UPS that can provide power to both single-phase and three-phase consumers. The general diagram of the UPS shown in Figure 1(a), close to that given in [14], [15], is considered. The converter under investigation Figure 1(b) consists of the following main elements: battery, isolated bidirectional DC-DC converter, for example in [16]–[18] bidirectional AC-DC converter, inductance (L), capacitance (C), and inductance (L) or LCL-filter providing electromagnetic compatibility of UPS with the grid and load.
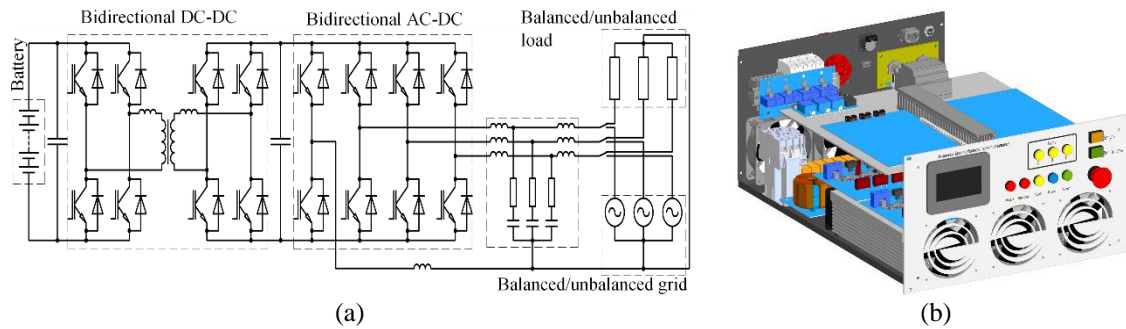
Figure 1. Electrical diagram of (a) power part and (b) UPS

A distinctive feature of the UPS in paper is the usage of a three-phase four-leg converter (3F4LC) as a bidirectional AC-DC converter, which provides both power to single-phase/three-phase consumers when the battery is discharging and constant voltage stabilization at the input of the DC-DC converter when it is charging. The subject of the article is a 3F4LC when operating in both inverter and rectifier modes. This element of the UPS has an important functional purpose and in addition, provides many quality indicators, for example: low voltage total harmonic distortion (THD) when operating in inverter mode, high power factor and low level of DC voltage pulsations in rectifier mode [15]. To date, a number of studies of such bidirectional converters are known for use in various applications, for example, as a shunt active power filter [19] including for operation as part of UPS. One of the most in-depth studies can be called [20], where on the basis of more than 400 sources different versions of structures, algorithms of space-vector pulse-width modulation (SVPWM), control and application of these converters are presented. Based on the analysis given in [20] and the power of the converter under investigation (up to 20 kW), it is proposed to investigate control algorithms on the example of the simplest two-level structure.

From the point of view of controlling a 3F4LC, the vast majority of publications are devoted to control in inverter mode, when the converter must provide power to a three-phase unbalanced and/or non-linear load when operating in autonomous mode. For example, [21] provides a number of works in which different coordinate systems are used for the designated class of converters for control to represent voltages and currents and accordingly, different types of current and voltage loop control: hysteresis control, finite-dimensional control with predictive model, control in sliding mode, proportional-integral, and proportional-resonance regulators. The closest to the control system developed in the model are algorithms with per-phase control of the converter [22], [23]. When the 3F4LC operates in rectifier mode, there is significantly less work. For example, publications [24], [25] are known. At the same time algorithms of control of three-phase three-leg active voltage rectifiers are developed quite well. Thus, algorithms with voltage vector orientation are most known [26] and direct power control [27]. The work proposes to develop a control algorithm based on a vector algorithm with voltage vector orientation, used in three-phase three-leg converters, taking into account adaptation to a four-leg structure.

The work is dedicated to the parametric study using computer modeling of the behavior of the 3F4LC when varying the parameters of the LCL filter and modulation frequency in order to optimize the mass and size characteristics of the converter while maintaining high power quality. Although there are relatively formalized methods for calculating the parameters of the LCL filter in both three-phase three-wire [28], [29], and four-wire systems [30], their application is somewhat heuristic. In many studies, the choice of parameters is primarily based on the requirements for filtering current and voltage, i.e., separating the frequency of the main harmonic of the generated voltage and the frequencies modulated by SVPWM, sometimes minimizing the pulsations of the DC link voltages and the battery charging current. However, the LCL filter provides not only filtering properties but also the potential for power factor correction and voltage control in rectifier mode due to energy storage in inductance. It should be taken into account that these same parameters determine the settings of the control system regulators and their achievable speed of response. Thus, it turns out that setting the parameters of the LCL filter is a task of multiparametric optimization, possessing significant complexity for analytical study. Therefore, the work presents a procedure for parametric modeling, taking into account the simplest control algorithms in different operating modes of the 3F4LC: inverter mode with symmetric and asymmetric load; and rectifier mode with balanced and unbalanced grid. The presented procedure allowed for the selection of optimal values of LCL filter parameters under conditions allowing variation of modulation frequency.

Thus, section 2 provides a mathematical description and models of a 3F4LC, as well as implemented computer models of control algorithms. In order to implement converter control algorithms when operating in inverter and rectifier modes, the algorithm of 3D SVPWM is also considered. In section 3, the effect of LCL filter parameters on the quality indicators of the 3F4LC is investigated when operating in inverter mode (THD of the generated current) and in rectifier mode (THD of the current consumed from the grid). Based on the results of mathematical modeling, conclusions are drawn about optimal values of LCL filter parameters providing bidirectional energy exchange.

2. THREE-PHASE FOUR-LEG CONVERTER CONTROL SYSTEM MODEL

The article discusses the control issues of 3F4LC operating in two different modes. The electrical diagram for the analysis of the inverter mode is shown in Figure 2(a), for the rectifier mode is shown in Figure 2(b). Both the load and the grid can generally may be unbalanced. In the electrical circuit of the power part of the converter, the following designations are introduced: $VT1$-$VT8$–power transistors, the state of which can be described by switching functions (if $S_x=0$, where $x \in \{a,b,c,n\}$, the transistor of the odd group of the corresponding phase is in the conducting state, and even in the non-conducting state, and vice versa at $S_x=1$); r_{Lf1}, L_{f1}, r_{Lf2}, and L_{f2} are the active and inductive resistance of the LCL filter choke on the converter and the grid side, respectively; r_{Cf} – current limiting resistance of capacitor; C_f – capacitance of LCL filter capacitor; r_n and L_n are the active and inductive resistance of the choke in the neutral; V_a, V_b, V_c, and V_n – potentials of middle points of the corresponding half-bridges of inverter; V_A, V_B, V_C, and V_N – voltage potentials at load; i_{abc}, i_{ABC}, and i_{Cabc} – three-phase currents through the choke (i_a, i_b, and i_c), load currents (i_A, i_B, and i_C) and capacitor currents (i_{Ca}, i_{Cb}, and i_{Cc}) of the LCL filter; i_n – neutral current; V_{dc} – DC voltage source; C_{dc} – DC link capacitance; u_A, u_B, and u_C are the three-phase grid voltages that can be both symmetrical and unsymmetric; Z – unbalanced three-phase load; and Z_L is the load of the rectifier.
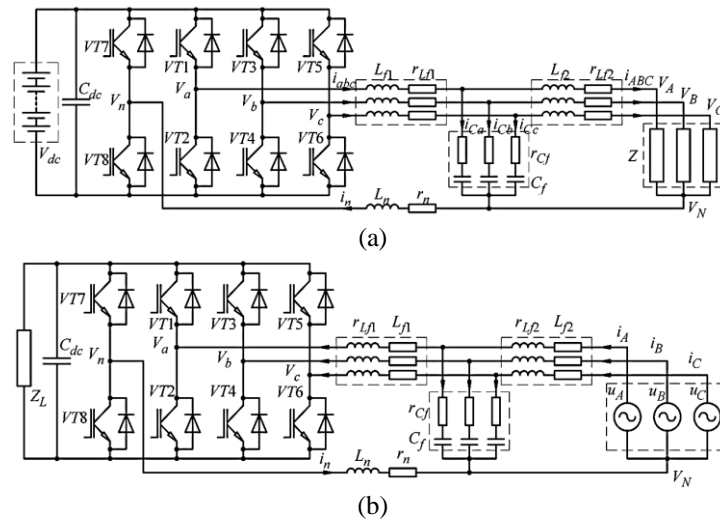

(a)

(b)

Figure 2. Electrical diagram of power part of 3F4LC during operation in two modes:
(a) inverter and (b) rectifier

2.1. Forming 3D PWM in αβγ coordinates

For independent generation of voltage of separate phases of 3F4LC during operation in inverter mode for unbalanced load (at unbalanced grid during operation in rectifier mode) 3D SVPWM is used, which has been developed and investigated in many works [31]–[35]. In the case of a 3F4LC, the balance conditions $-V_{AN}+V_{BN}+V_{CN}=0$ may be disturbed. In this case, it is also possible to perform a transformation to an orthogonal fixed coordinate system, but no longer two, but three-phase in space αβγ, defined in this case by Clarke transformation. For the 3F4LC shown in Figure 2, depending on the state of the power transistors $VT1$-$VT8$ determined by the switching function S_x, 16 basic voltage vectors shown in Figure 3(a) in αβγ space using Clarke transformation; Figure 3(b) projections of vectors on plane αβ and AB, respectively; and Figure 3(c) in ABC space. In addition, Table 1 [31] shows the correspondence of the states of the power transistors described by the generalized switching function (in $S_a\ S_b\ S_c\ S_n$ format), vectors and voltage values in relative units obtained by dividing by voltage V_{dc}.
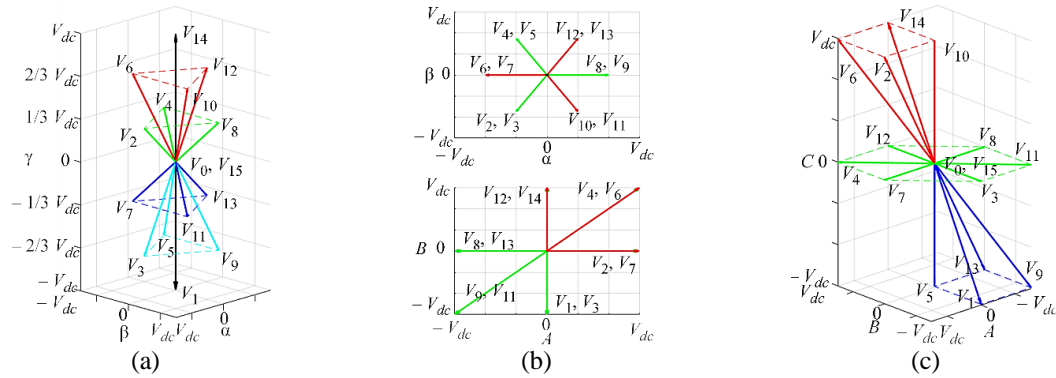
Figure 3. Position of 16 basic voltage vectors in space: (a) in space αβγ; (b) projections of vectors on plane αβ and AB, respectively; and (c) in ABC space

Table 1. Correspondence of states/vectors and voltages of 3F4LC

States ($S_aS_bS_cS_n$)	Vectors	V_a, pu	V_b, pu	V_c, pu	V_α, pu	V_β, pu	V_γ, pu
0000	V_0	0	0	0	0	0	0
0001	V_1	−1	−1	−1	0	0	−1
0010	V_2	0		1	−1/3	−$\sqrt{3}$/3	1/3
0011	V_3	−1	−1	0	−1/3	−$\sqrt{3}$/3	−2/3
0100	V_4	0	1	0	−1/3	$\sqrt{3}$/3	1/3
0101	V_5	−1	0	−1	−1/3	$\sqrt{3}$/3	−2/3
0110	V_6	0	1	1	−2/3	0	2/3
0111	V_7	−1	0	0	−2/3	0	−1/3
1000	V_8	1	0	0	2/3	0	1/3
1001	V_9	0	−1	−1	2/3	0	−2/3
1010	V_{10}	1	0	1	1/3	−$\sqrt{3}$/3	2/3
1011	V_{11}	0	−1	0	1/3	−$\sqrt{3}$/3	−1/3
1100	V_{12}	1	1	0	1/3	$\sqrt{3}$/3	2/3
1101	V_{13}	0	0	−1	1/3	$\sqrt{3}$/3	−1/3
1110	V_{14}	1	1	1	0	0	1
1111	V_{15}	0	0	0	0	0	0

When considering the basic voltage vectors in space αβγ their projection onto the αβ plane is a regular hexagon divided into six sectors, as in the case of a three-phase three-leg converter. However, the procedure of forming 3D SVPWM is a more laborious process because each sector shown on the αβ plane in space defines a triangular prism containing four tetrahedrons whose faces are formed by space vectors in the prism. In the case of a 3F4LC, there are 24 combinations of three non-zero and one/two zero vectors. In general, the 3D SVPWM generation process consists of the following main steps: i) Converting a given vector from ABC to αβγ using the Clarke transform; ii) Determining a prism and a tetrahedron within which a predetermined transformed voltage vector is located; and iii) Determining the transistor switching sequence and the on time of each vector defining the vertices of the selected tetrahedron.

The procedure for selecting the desired tetrahedron in the αβγ space is intensive and poorly formalized. At the same time, [31] shows that the selection of vectors defining tetrahedrons in ABC space can be carried out quite simply on the basis of comparison of setting voltages instantaneous values for individual phases, as shown in Table 2 [31]–[36]. The set of vectors required to form a reference vector does not depend on the selection of the coordinate system. According to [36], with a known tetrahedron, the relative start times of each non-zero state is defined as (1).

$$[d_1 \quad d_2 \quad d_3]^T = T_d/V_{dc} \left[V_\alpha^{ref} \ V_\beta^{ref} \ V_\gamma^{ref} \right]^T \tag{1}$$

Where d_1, d_2, and d_3 are relative inclusion times of non-zero vectors corresponding to tetrahedron faces; T_d is a transformation matrix individual for each tetrahedron and defined in Table 2; V_α^{ref}, V_β^{ref}, and V_γ^{ref} are projections of a reference voltage vector on the axis of a three-phase orthogonal αβγ coordinate system. The relative inclusion time of the zero vectors d_0 is determined considering as (1) as $d_0 = 1 - d_1 - d_2 - d_3$. When implementing the 3D SVPWM algorithm, a symmetric sequence of inclusion of vectors within one SVPWM period is used in the computer model.

Table 2. Determination of a tetrahedron by the ratio of specified voltages

Tetrahedron	Condition	T_d	Tetrahedron	Condition	T_d
$T(V_1, V_3, V_7)$	$0 \geq V_c \geq V_b \geq V_a$	$\begin{bmatrix} 1/2 & \sqrt{3}/2 & -1 \\ 0 & -\sqrt{3} & 0 \\ -3/2 & \sqrt{3}/2 & 0 \end{bmatrix}$	$T(V_4, V_5, V_7)$	$V_b \geq 0 \geq V_c \geq V_a$	$\begin{bmatrix} -1/2 & \sqrt{3}/2 & 1 \\ 1/2 & \sqrt{3}/2 & -1 \\ -3/2 & -\sqrt{3}/2 & 0 \end{bmatrix}$
$T(V_1, V_3, V_{11})$	$0 \geq V_c \geq V_a \geq V_b$	$\begin{bmatrix} 1/2 & \sqrt{3}/2 & -1 \\ -3/2 & -\sqrt{3}/2 & 0 \\ 3/2 & -\sqrt{3}/2 & 0 \end{bmatrix}$	$T(V_4, V_5, V_{13})$	$V_b \geq 0 \geq V_a \geq V_c$	$\begin{bmatrix} -1/2 & \sqrt{3}/2 & 1 \\ -1 & 0 & -1 \\ 3/2 & \sqrt{3}/2 & 0 \end{bmatrix}$
$T(V_1, V_5, V_7)$	$0 \geq V_b \geq V_c \geq V_a$	$\begin{bmatrix} 1/2 & -\sqrt{3}/2 & -1 \\ 0 & \sqrt{3} & 0 \\ -3/2 & -\sqrt{3}/2 & 0 \end{bmatrix}$	$T(V_4, V_6, V_7)$	$V_b \geq V_c \geq 0 \geq V_a$	$\begin{bmatrix} 0 & \sqrt{3} & 0 \\ -1/2 & -\sqrt{3}/2 & 1 \\ -1 & 0 & -1 \end{bmatrix}$
$T(V_1, V_5, V_{13})$	$0 \geq V_b \geq V_a \geq V_c$	$\begin{bmatrix} 1/2 & -\sqrt{3}/2 & -1 \\ -3/2 & \sqrt{3}/2 & 0 \\ 3/2 & \sqrt{3}/2 & 0 \end{bmatrix}$	$T(V_4, V_6, V_{14})$	$V_b \geq V_c \geq V_a \geq 0$	$\begin{bmatrix} 0 & \sqrt{3} & 0 \\ -3/2 & -\sqrt{3}/2 & 0 \\ 1 & 0 & 1 \end{bmatrix}$
$T(V_1, V_9, V_{11})$	$0 \geq V_a \geq V_c \geq V_b$	$\begin{bmatrix} -1 & 0 & -1 \\ 3/2 & \sqrt{3}/2 & 0 \\ 0 & -\sqrt{3} & 0 \end{bmatrix}$	$T(V_4, V_{12}, V_{13})$	$V_b \geq V_a \geq 0 \geq V_c$	$\begin{bmatrix} -3/2 & \sqrt{3}/2 & 0 \\ 1 & 0 & 1 \\ 1/2 & \sqrt{3}/2 & -1 \end{bmatrix}$
$T(V_1, V_9, V_{13})$	$0 \geq V_a \geq V_b \geq V_c$	$\begin{bmatrix} -1 & 0 & -1 \\ 3/2 & -\sqrt{3}/2 & 0 \\ 0 & \sqrt{3} & 0 \end{bmatrix}$	$T(V_4, V_{12}, V_{14})$	$V_b \geq V_a \geq V_c \geq 0$	$\begin{bmatrix} -3/2 & \sqrt{3}/2 & 0 \\ 3/2 & \sqrt{3}/2 & 0 \\ -1/2 & -\sqrt{3}/2 & 1 \end{bmatrix}$
$T(V_2, V_3, V_7)$	$V_c \geq 0 \geq V_b \geq V_a$	$\begin{bmatrix} -1/2 & -\sqrt{3}/2 & 1 \\ 1/2 & -\sqrt{3}/2 & -1 \\ -3/2 & \sqrt{3}/2 & 0 \end{bmatrix}$	$T(V_8, V_9, V_{11})$	$V_a \geq 0 \geq V_c \geq V_b$	$\begin{bmatrix} 1 & 0 & 1 \\ 1/2 & \sqrt{3}/2 & -1 \\ 0 & -\sqrt{3} & 0 \end{bmatrix}$
$T(V_2, V_3, V_{11})$	$V_c \geq 0 \geq V_a \geq V_b$	$\begin{bmatrix} -1/2 & -\sqrt{3}/2 & 1 \\ -1 & 0 & -1 \\ 3/2 & -\sqrt{3}/2 & 0 \end{bmatrix}$	$T(V_8, V_9, V_{13})$	$V_a \geq 0 \geq V_b \geq V_c$	$\begin{bmatrix} 1 & 0 & 1 \\ 1/2 & \sqrt{3}/2 & -1 \\ 0 & \sqrt{3} & 0 \end{bmatrix}$
$T(V_2, V_6, V_7)$	$V_c \geq V_b \geq 0 \geq V_a$	$\begin{bmatrix} 0 & -\sqrt{3} & 0 \\ -1/2 & \sqrt{3}/2 & 1 \\ -1 & 0 & -1 \end{bmatrix}$	$T(V_8, V_{10}, V_{11})$	$V_a \geq V_c \geq 0 \geq V_b$	$\begin{bmatrix} 3/2 & \sqrt{3}/2 & 0 \\ -1/2 & -\sqrt{3}/2 & 1 \\ 1/2 & -\sqrt{3}/2 & -1 \end{bmatrix}$
$T(V_2, V_6, V_{14})$	$V_c \geq V_b \geq V_a \geq 0$	$\begin{bmatrix} 0 & -\sqrt{3} & 0 \\ -3/2 & \sqrt{3}/2 & 0 \\ 1 & 0 & 1 \end{bmatrix}$	$T(V_8, V_{10}, V_{14})$	$V_a \geq V_c \geq V_b \geq 0$	$\begin{bmatrix} 3/2 & \sqrt{3}/2 & 0 \\ 0 & -\sqrt{3} & 0 \\ -1/2 & \sqrt{3}/2 & 1 \end{bmatrix}$
$T(V_2, V_{10}, V_{11})$	$V_c \geq V_a \geq 0 \geq V_b$	$\begin{bmatrix} -3/2 & -\sqrt{3}/2 & 0 \\ 1 & 0 & 1 \\ 1/2 & -\sqrt{3}/2 & -1 \end{bmatrix}$	$T(V_8, V_{12}, V_{13})$	$V_a \geq V_b \geq 0 \geq V_c$	$\begin{bmatrix} 3/2 & -\sqrt{3}/2 & 0 \\ -1/2 & \sqrt{3}/2 & 1 \\ 1/2 & \sqrt{3}/2 & -1 \end{bmatrix}$

2.2. General description of per-phase voltage control system of three-phase four-leg voltage source inverter

To obtain a mathematical model of a three-phase four-leg voltage source inverter (3F4L VSI), Figure 4 shows a diagram of one phase of its output circuit and we assume that r_{Lf2} and L_{f2} are included in the Z_A load to simplify calculations. The voltage balance equation written for one phase using Kirchhoff's voltage law can be represented by (2).

$$u_{an} = r_{Lf}i_a + L_f \frac{di_a}{dt} + u_{AN} - r_n i_n - L_n \frac{di_n}{dt} \tag{2}$$

Where $u_{an} = V_a - V_n$–potential difference of middle point of phase A half-bridge of 3F4L VSI and half-bridge of neutral-forming conductor; $u_{Lf} = r_{Lf}i_a + L_f(di_a/dt)$–voltage drop across the filter choke LCL from the inverter side; u_{AN} – voltage drop at one load phase (including $u_{Lf2} = r_{Lf2}i_a + L_{f2}(di_a/dt)$); $u_{Ln} = r_n i_n + L_n(di_n/dt)$ – voltage drop at the neutral current limiting choke. Using Kirchhoff's law of currents, you can also write (3).

$$i_{Ca} = i_a - i_A \ \Rightarrow \ C_f \frac{du_{CA}}{dt} = i_a - i_A \tag{3}$$

Where u_{CA} is the voltage drop across the filter capacitor LCL similar to (2) and (3), a general mathematical description of a 3F4L VSI can be made taking into account the active resistance of the filter capacitor LCL.
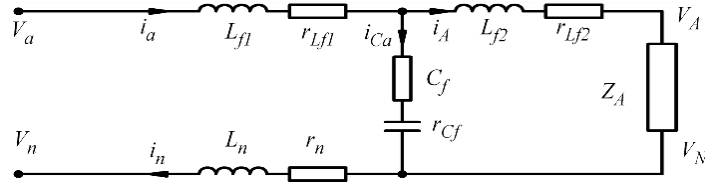
Figure 4. Electrical diagram of one phase of 3F4L VSI

Thus, the mathematical model of the 3F4L VSI in terms of control theory is a multi-coupled multiple input and multiple output (MIMO) system. The system that shown in (4) can be represented by a system of differential equations of six independent state variables, as which it is convenient to take three-phase systems of currents through the choke and voltages on the LCL filter capacitor. In this case, the purpose of the control is to stabilize voltages at individual load phases under conditions of uncertainty of nature (active and/or active-reactive, single-phase and/or three-phase, and linear and/or non-linear) and load values within the available power. Since the regulation of an interconnected MIMO system is of considerable complexity, approaches to transforming the mathematical description in such a way as to proceed to the consideration of three independent single-input single-output (SISO) systems are considered. Next, consider the option of switching to a SISO system in order to implement per-phase load voltage control of the 3F4L VSI. To switch to the isolated mathematical model of the 3F4L VSI according to [21], a description in state space is drawn up, provided that the $L_n = L_{f1}/2 = L/2, r_{Cf} = r_{Lf} = r_n = R$, of the type.

$$
\begin{cases}
\begin{bmatrix} u_{an} \\ u_{bn} \\ u_{cn} \end{bmatrix} = \begin{bmatrix} u_{AG} \\ u_{BG} \\ u_{CG} \end{bmatrix} + r_{Lf} \begin{bmatrix} i_a \\ i_b \\ i_c \end{bmatrix} + L_f \frac{d}{dt} \begin{bmatrix} i_a \\ i_b \\ i_c \end{bmatrix} - r_n \begin{bmatrix} i_n \\ i_n \\ i_n \end{bmatrix} + L_n \frac{d}{dt} \begin{bmatrix} i_n \\ i_n \\ i_n \end{bmatrix} \\
C_f \frac{d}{dt} \begin{bmatrix} u_{CA} \\ u_{CB} \\ u_{CC} \end{bmatrix} = \begin{bmatrix} i_a \\ i_b \\ i_c \end{bmatrix} - \begin{bmatrix} i_A \\ i_B \\ i_C \end{bmatrix}
\end{cases}
\tag{4}
$$

Where $\mathbf{x} = [i_a \quad u_{CA} \quad i_b \quad u_{CB} \quad i_c \quad u_{CC}]^T \in R^6$ is a vector of variables of a state as which the three-phase currents through a choke and voltage on the LCL filter capacitor, i.e. are accepted $\mathbf{u} = [u_{an} \quad u_{bn} \quad u_{cn}]^T \in R^3$ is the input vector represented by the potential difference between the mid-points of the half-bridges of the 3F4L VSI and the mid-point of the neutral half-bridge; $w = [i_A \quad i_B \quad i_C]^T \in R^3$ is a vector of disturbances represented by load currents. In [21], it is proposed to proceed to the consideration of three SISO systems by compensating for cross-links between phases. As can be seen from the system in (5), each derivative of the phase choke current of the 3F4L VSI depends only on this current itself and the voltages on all three capacitors of the LCL filter.

$$
\dot{\mathbf{x}} = \begin{bmatrix}
\frac{-2R}{L} & \frac{-4}{5L} & 0 & \frac{1}{5L} & 0 & \frac{1}{5L} \\
\frac{1}{C_f} & 0 & 0 & 0 & 0 & 0 \\
0 & \frac{1}{5L} & \frac{-2R}{L} & \frac{-4}{5L} & 0 & \frac{1}{5L} \\
0 & 0 & \frac{1}{C_f} & 0 & 0 & 0 \\
0 & \frac{1}{5L} & 0 & \frac{1}{5L} & \frac{-2R}{L} & \frac{-4}{5L} \\
0 & 0 & 0 & 0 & \frac{1}{C_f} & 0
\end{bmatrix} \mathbf{x}
+ \begin{bmatrix}
\frac{4}{5L} & \frac{-1}{5L} & \frac{-1}{5L} \\
0 & 0 & 0 \\
\frac{-1}{5L} & \frac{4}{5L} & \frac{-1}{5L} \\
0 & 0 & 0 \\
\frac{-1}{5L} & \frac{-1}{5L} & \frac{4}{5L} \\
0 & 0 & 0
\end{bmatrix} \mathbf{u}
+ \begin{bmatrix}
\frac{4R}{5L} & \frac{-1R}{5L} & \frac{-1R}{5L} \\
\frac{-1}{C_f} & 0 & 0 \\
\frac{-R}{5L} & \frac{4R}{5L} & \frac{-R}{5L} \\
0 & \frac{-1}{C_f} & 0 \\
\frac{-R}{5L} & \frac{-R}{5L} & \frac{4R}{5L} \\
0 & 0 & \frac{-1}{C_f}
\end{bmatrix} \mathbf{w}
\tag{5}
$$

$$
\begin{bmatrix} u_{an} \\ u_{bn} \\ u_{cn} \end{bmatrix} = \begin{bmatrix} u_{an}^{ref} + k_1 u_{CB} + k_2 u_{CC} \\ u_{bn}^{ref} + k_3 u_{CA} + k_4 u_{CC} \\ u_{cn}^{ref} + k_5 u_{CA} + k_6 u_{CB} \end{bmatrix}
$$

At the same time derivative of choke current of any phase does not depend on currents of other phases. Under these conditions, it is proposed to generate a control effect u so as to compensate for the voltages of the LCL filter capacitors in other phases. Where $k_1 = k_2 = k_3 = k_4 = k_5 = k_6 = -1/3$ – coefficients that provide compensation for cross-links between phases; $u_{an}^{ref}, u_{bn}^{ref}$, and u_{cn}^{ref} – reference values of inverter output

voltages ensuring stabilization of load voltages. Based on the mathematical description [21], the control system given in Figure 5 is proposed, where the following designations are introduced: voltage sensor (VS); proportional-integral (PI) regulator; proportional (P) regulator; $\alpha\beta \rightarrow dq$ and $dq \rightarrow \alpha\beta$ – coordinate transformations; ωt_k – instantaneous phase value of capacitor voltage of corresponding phase k ($k \in \{A, B, C\}$); u_{kd}, u_{kq}, and $u_{k\alpha}$, $u_{k\beta}$– an analogue of the projection of the voltage vector for the corresponding phase on the axis of the rotating and fixed coordinate system, respectively.
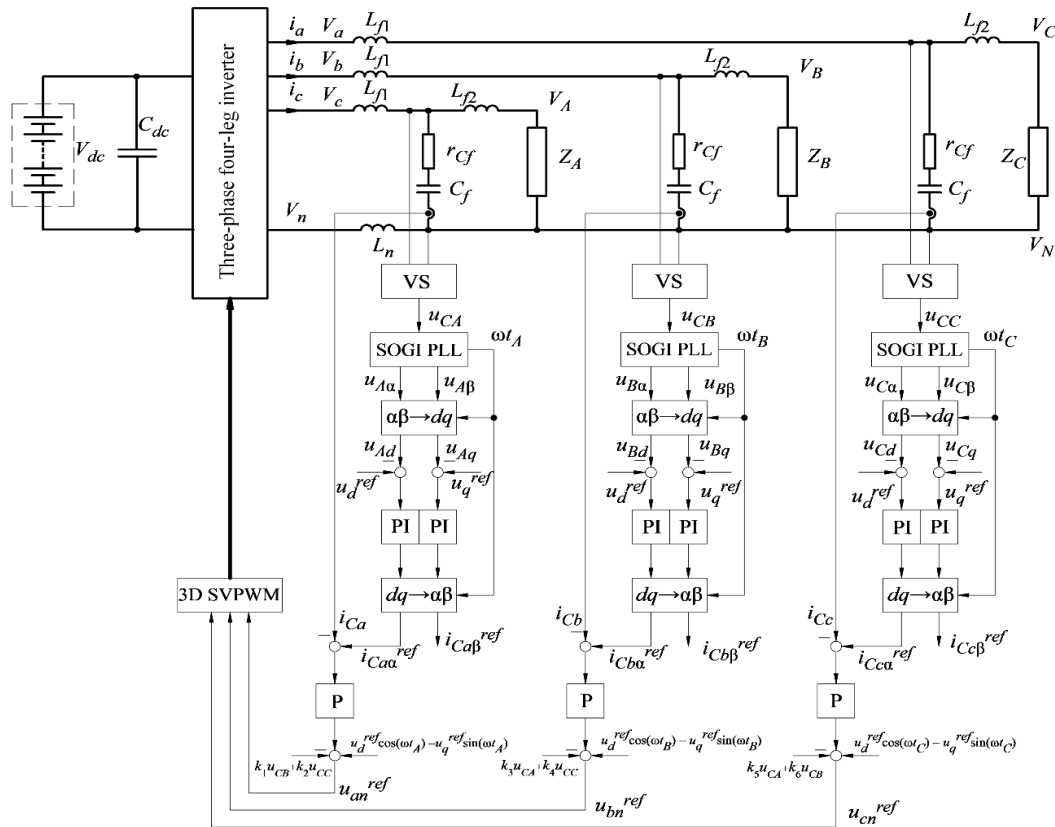
Figure 5. Functional diagram of 3F4L VSI control system

The control system [23] has a feature that is that the single-phase voltage control circuit is made in the rotating dq coordinate system. To obtain phase voltage projections on the axis of this coordinate system, a known Park transform applied to three-phase voltage systems is generally used. In this case, Park transformation allows to convert the initial system of three-phase signals changing according to harmonic law to the system of two constant signals for which there are developed methods of synthesis of control algorithms and adjustment of their parameters. Since the control system under consideration is built separately for each phase, it is not possible to use the Park transformation directly to obtain u_α and u_β. It is proposed to obtain these components artificially using one of the modifications of the second-order generalized integrator with phase-locked loop (SOGI-PLL). The use of SOGI-PLL makes it possible to generate a signal shifted from the input by 90 electronic degrees, the same amplitude and frequency. Output voltage is controlled by means of PI-regulator by obtained phase voltages in projections on axis of rotating dq coordinate system. PI controllers in the rotating coordinate system ensure the equality of u_{kd} and u_{kq} components, given u_d^{ref} and u_q^{ref} values, which can be obtained by applying the Park transformation directly to the desired u_{ABC} voltage system. In this case, the u_d^{ref} will correspond to the amplitude value of the generated voltage, and the u_q^{ref} will be zero.

Output of PI-regulator will be used as setting action for P-regulator of current in fixed coordinate system of $\alpha\beta$. A voltage setting signal of a separate phase is generated at the output of the P-current regulator. At the same time, a signal is additionally added to the output of the P-regulator, which allows to compensate for the presence of cross-links. The article conducted a study of the operability of the given algorithm at balanced and unbalanced load. Values of parameters of control system regulators and simulation diagrams are given in Table 3. The results of modeling are given in Figure 6(a) without control system and in

Figure 6(b) with control system. In the initial state, the inverter operates on a three-phase balanced load with a nominal phase voltage of 220 V at 50 Hz and active power of 10 kW. Then, at a time of 0.5 s, a single-phase load of 10 kW of active power is added parallel to phase A, and at 0.6 s, a load with an active (20 kW) and reactive (10 kVAR) power is added to phase C.

Table 3. Parameters of control system and simulation circuit by 3F4L VSI

Regulator	Parameters	Value	
SOGI	Proportional component	0.8	
SOGI-PLL	Proportional/integral component	10	30
Voltage PI-regulator	Proportional/integral component	0.2	30
	Saturation of integral component	± 350	
Current P-regulator	Proportional component	1	
LCL-filter	Inductive resistance of the inverter/grid side choke, L	400 uH	
	Active resistance of the inverter/grid side choke, R	10 mOhm	
	Capacitance of capacitor, C	10 uF	
	Active resistance of capacitor, R	10 Ohm	
Battery	Nominal voltage, V	550 V	
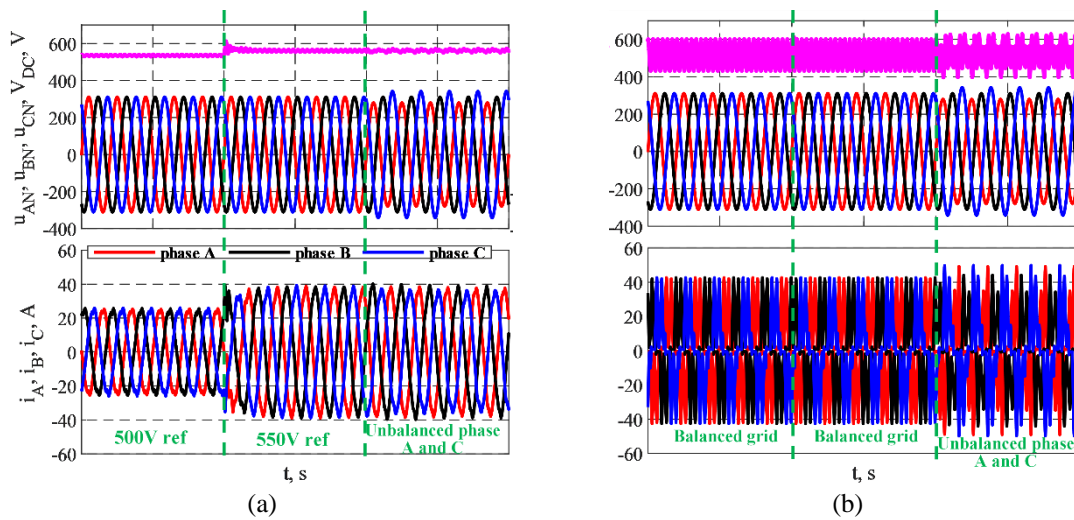
Figure 6. Comparison of operation of 3F4L VSI (a) without control system and (b) with control system

2.3. Description of three-phase four-leg rectifier

When compiling a computer model, a classic three-phase three-leg converter control system described, for example, in [37] is used as a basic structure. In order to adapt it to the four-leg scheme, it is necessary to draw up a mathematical description in a natural coordinate system according to a method similar to that used in subsection 2.2, after which the Park transformation is carried out to an orthogonal rotating coordinate system. However, unlike [37], where the mathematical model of the three-phase active rectifier is reduced to fa two-phase orthogonal coordinate system, in the investigated case four-leg rectifier model is reduced to a three-phase rotating orthogonal system $dq0$, where the projection on the 0 axis is not equal to zero. In this case, it is proposed to use, by analogy with [25], an additional independent current circuit with a regulator, the purpose of which is to minimize the $i_0 \rightarrow 0$ current component. Figure 7 shows the functional diagram of the modified three-phase four-leg active voltage rectifier (3F4L AVR) control system taking into account the current control circuit of the projection on the zero axis, where the following designations are introduced: ABC $\rightarrow$ $dq0$ and $dq0 \rightarrow$ ABC – direct and reverse conversion of state variables from the natural coordinate system to the rotating and back; PIv – proportional-integrating voltage regulator; and proportional-integrating current (PIc) regulator.

Control system of 3F4L AVR is built according to subordinate control principle and has current and voltage circuit. Internal current circuit sets dynamics of transient processes of i_d, i_q, and i_0 and limits maximum value of current consumed from grid. The external voltage circuit stabilizes the level of the output rectified voltage. Setting up these regulators is not subject to article consideration. Parameters of 3F4L AVR control system are given in Table 4. The results of modeling are given in Figure 8(a) with control system and in Figure 8(b) without control system. Both models are studied in two modes: when operating with a balanced grid (in two different mode in case with control: 500 V and 550 V in the DC link); operating with unbalanced grid.
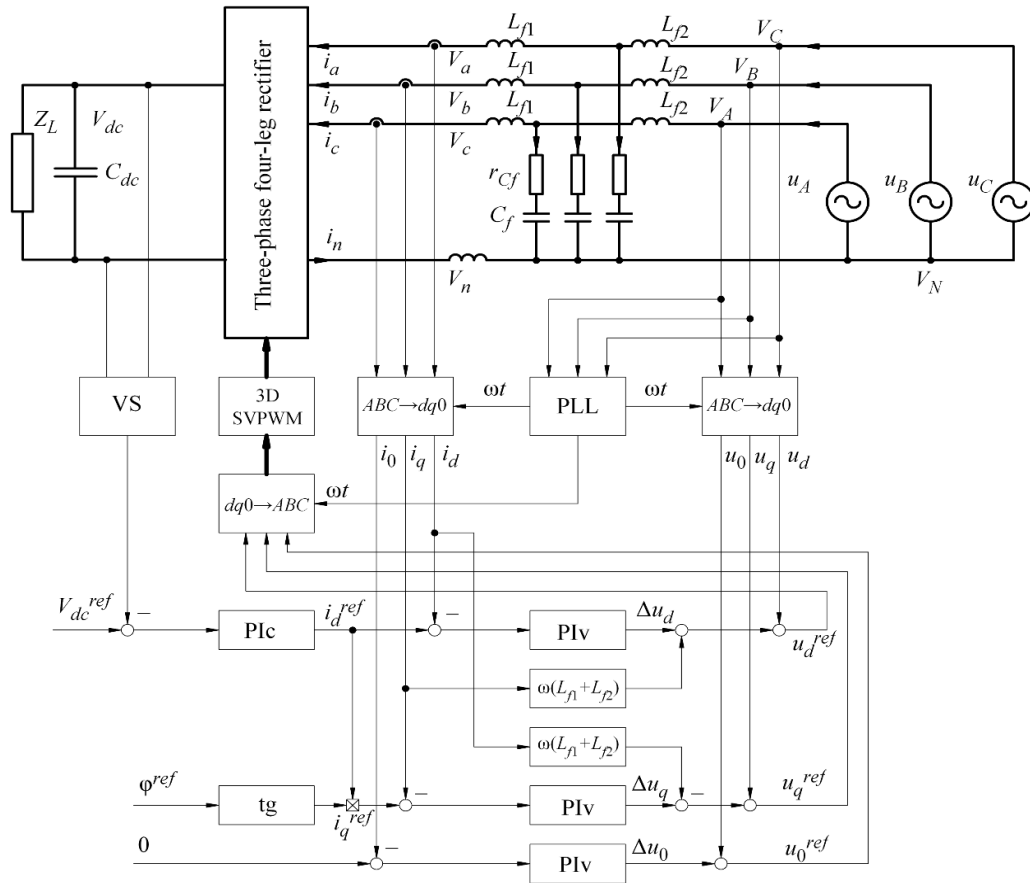
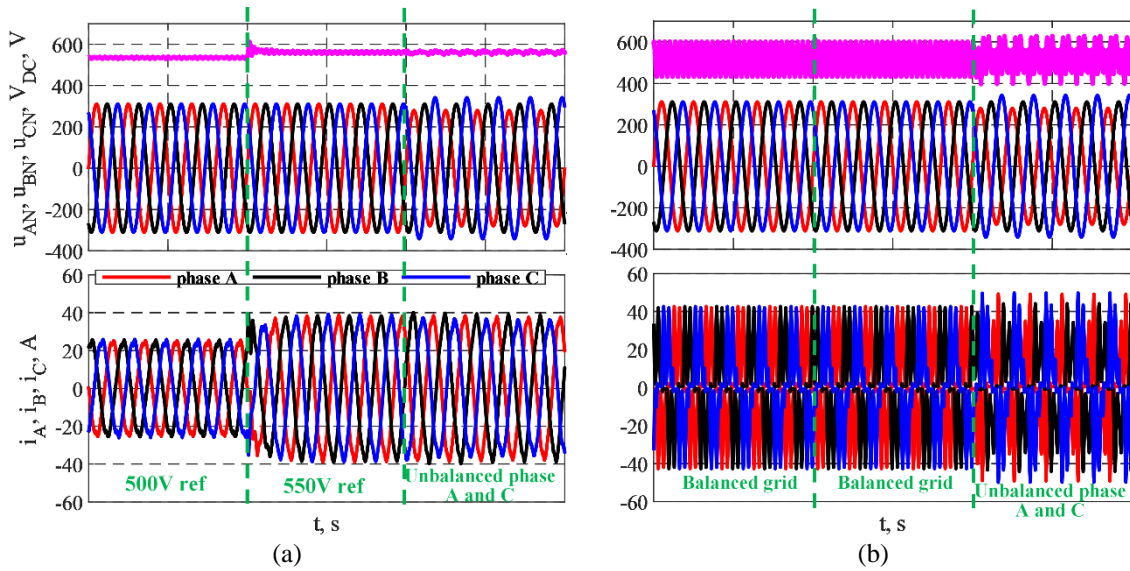Figure 7. Functional diagram of the control system of the 3F4L AVR

Figure 8. Comparison of operation of 3F4L AVR (a) with control system and (b) without control system

Table 4. Control system parameters and 3F4L AVR modeling diagrams

Regulator	Parameters	Value	
Voltage PI-regulator	Proportional/integral component	0.0019	0.0088
Current PI-regulator	Proportional/integral component	0.000564	0.000883
	Saturation of integral component	± 1000	
DC-link	Active load resistance	25 Ohm	
	DC link filter capacity	120 uF	

3. RESULTS AND DISCUSSION

As a result of computer modeling for the studied control algorithms, an empirical dependence was revealed on the influence of the LCL filter parameters and modulation frequency on the performance quality of the 3F4LC in various operating modes. In rectifier mode, changes in the modulation frequency and the capacitance value of the LCL filter have an insignificant impact on the quality of consumed electric power, whereas changing the inductances has the opposite effect. It should be noted that reducing the inductances to a certain threshold value allows for the improvement of the consumed current quality, while increasing them in some cases leads to a loss of stability of the control algorithm. Taking into account the need to ensure quality during bidirectional energy conversion, it appears that in inverter mode, one can affect the modulation frequency and LCL filter capacitance without significant loss of quality in rectifier mode, as confirmed by the results of the modeling. The results of computer simulation with the given parameters of the LCL filter are presented in Figure 9. With this combination of parameters, it was possible to achieve a current THD of 6.5% when operating in rectifier mode and 6% in inverter mode.
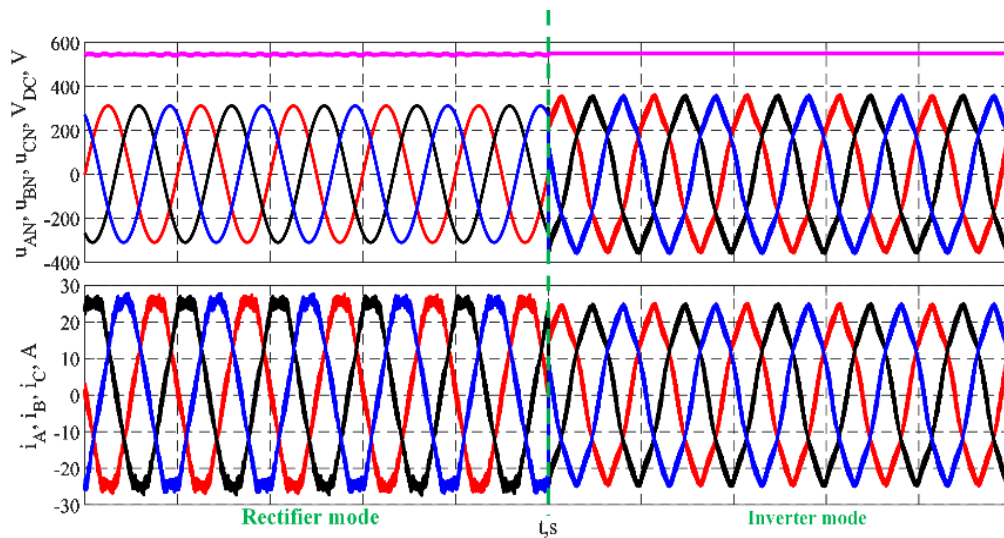
Figure 9. 3F4LC operation in bidirectional mode

Figure 10 shows the results of a study of the current THD on the grid side (consumed in rectifier mode (blue surface) and generated in inverter mode (red surface)) in the form of a series of surfaces at 4 fixed capacitance values: 30 nF; 300 nF; 3 µF and 30 µF, 4 fixed values of converter modulation frequencies: 5 kHz, 10 kHz, 20 kHz, and 40 kHz and with inductance variations on both the grid and the converter side in the range from 100 to 800 µH. Thus, Figure 10 shows the results for the following fixed parameter values; Figure 10(a): C = 30 nF, f_{PWM} = 5 kHz, Figure 10(b): C = 300 nF, f_{PWM} = 5 kHz, Figure 10(c): C = 3 µF, f_{PWM} = 5 kHz, Figure 10(d): C = 30 µF, f_{PWM} = 5 kHz, Figure 10(e): C = 30 nF, f_{PWM} = 10 kHz, Figure 10(f): C = 300 nF, f_{PWM} = 10 kHz, Figure 10(g): C = 3 µF, f_{PWM} = 10 kHz, Figure 10(h): C = 30 µF, f_{PWM} = 10 kHz, Figure 10(i): C = 30 nF, f_{PWM} = 20 kHz, Figure 10(j): C = 300 nF, f_{PWM} = 20 kHz, Figure 10(k): C = 3 µF, f_{PWM} = 20 kHz, Figure 10(l): C = 30 µF, f_{PWM} = 20 kHz, Figure 10(m): C = 30 nF, f_{PWM} = 40 kHz, Figure 10(n): C = 300 nF, f_{PWM} = 40 kHz, Figure 10(o): C = 3 µF, f_{PWM} = 40 kHz, and Figure 10(p): C = 30 µF, f_{PWM} = 40 kHz.

The ranges of values of capacitance, inductance and switching frequency are selected in order to minimize the weight and size indicators of the LCL filter when developing the UPS with a rated power of 10 kW while maintaining filtering properties. In this case, a value of less than 8% is taken as a satisfactory current THD. Analysis of the given graphs indicates that at a frequency of 20 kHz, show in Figures 10(i)-(l) it is possible not only to achieve the declared current quality, but also to minimize the weight and size indicators of the LCL filter. At high switching frequencies, shown in Figures 10(m)-10(p) in inverter mode, a THD limit of 2-3% is reached. It is obvious that the reduction in THD is affected by both the switching frequency and the capacitance value, but only in inverter mode, and in rectifier mode these two parameters, especially capacitance, make virtually no significant changes. For the developed UPS with a power of 10 kW, it is proposed to choose an inductance of 375 µH, which falls within the range of optimal values (300 µH-400 µH), a capacitance of 3.3 µF at a switching frequency of 20 kHz.

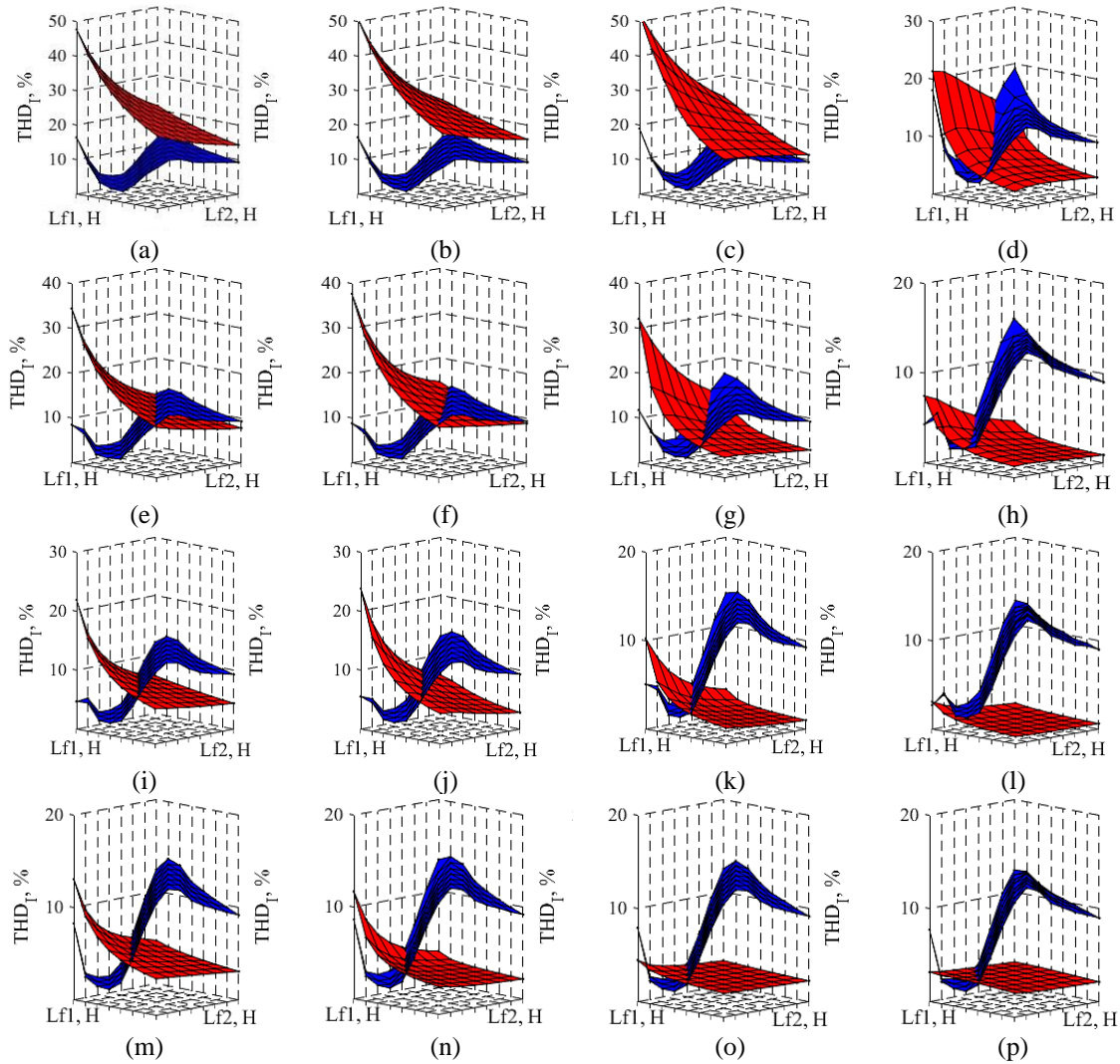Figure 10. Analysis of current quality with variable parameters of the LCL filter: (a) C = 30 nF, f_{PWM} = 5 kHz; (b) C = 300 nF; f_{PWM} = 5 kHz; (c) C = 3 μF, f_{PWM} = 5 kHz; (d) C = 30 μF, f_{PWM} = 5 kHz; (e) C = 30 nF, f_{PWM} = 10 kHz; (f) C = 300 nF, f_{PWM} = 10 kHz, (g) C = 3 μF, f_{PWM} = 10 kHz; (h) C = 30 μF, f_{PWM} = 10 kHz; (i) C = 30 nF, f_{PWM} = 20 kHz; (j) C = 300 nF, f_{PWM} = 20 kHz; (k) C = 3 μF, f_{PWM} = 20 kHz; (l) C = 30 μF, f_{PWM} = 20 kHz; (m) C = 30 nF, f_{PWM} = 40 kHz; (n) C = 300 nF, f_{PWM} = 40 kHz; (o) C = 3 μF, f_{PWM} = 40 kHz; and (p) C = 30 μF, f_{PWM} = 40 kHz

4.   CONCLUSION

In this study, control algorithms for a 3F4LC operating in both inverter and rectifier modes using 3D PWM were investigated and implemented in the form of computer models. A significant challenge in calculating the parameters of control systems using known methods was the inclusion of an LCL filter, whose elements perform different functions in various modes. Therefore, this study initially conducted a preliminary assessment of the LCL filter parameters. Subsequently, using the developed computer model, a comprehensive analysis was performed to examine the impact of the LCL filter parameters and modulation frequency on the quality metrics (total harmonic distortion of the grid/load current) of the 3F4LC's operation in both inverter and rectifier modes. The aim was to identify optimal parameter values that ensure acceptable quality during bidirectional energy exchange. The research findings were applied to design a physical prototype of a 10 kW grid UPS.

Further development of research is aimed at a more in-depth study of the parallel operation modes of similar electrical energy storage devices with their own bidirectional converters, installed at a considerable distance from each other and included in a smart grid without additional switching equipment, as well as analytical and numerical studying the influence of LCL filter parameters on the processes of synchronization

and power distribution loads, as well as minimizing weight and dimensions while maintaining both system stability and power quality indicators.

ACKNOWLEDGEMENTS

REFERENCES

[1] P. K. Dubey, B. Singh, V. Kumar, and D. Singh, "A novel approach for comparative analysis of distributed generations and electric vehicles in distribution systems," *Electrical Engineering*, Oct. 2023, doi: 10.1007/s00202-023-02072-2.

[2] B. Singh and P. K. Dubey, "Distributed power generation planning for distribution networks using electric vehicles: Systematic attention to challenges and opportunities," *Journal of Energy Storage*, vol. 48, p. 104030, Apr. 2022, doi: 10.1016/j.est.2022.104030.

[3] P. K. Dubey, B. Singh, D. K. Patel, and D. Singh, "Distributed Generation Current Scenario in the World," *International Journal For Multidisciplinary Research*, vol. 5, no. 4, Jul. 2023, doi: 10.36948/ijfmr.2023.v05i04.4625.

[4] B. Singh, P. K. Dubey, and S. N. Singh, "Recent Optimization Techniques for Coordinated Control of Electric Vehicles in Super Smart Power Grids Network: A State of the Art," in *2022 IEEE 9th Uttar Pradesh Section International Conference on Electrical, Electronics and Computer Engineering (UPCON)*, IEEE, Dec. 2022, pp. 1–7, doi: 10.1109/UPCON56432.2022.9986471.

[5] N. Padmawansa, K. Gunawardane, S. Madanian, and A. M. Than, "Battery Energy Storage Capacity Estimation for Microgrids Using Digital Twin Concept," *Energies*, vol. 16, no. 12, p. 4540, Jun. 2023, doi: 10.3390/en16124540.

[6] N. Blasuttigh, S. Negri, A. M. Pavan, and E. Tironi, "Optimal Sizing and Environ-Economic Analysis of PV-BESS Systems for Jointly Acting Renewable Self-Consumers," *Energies*, vol. 16, no. 3, p. 1244, Jan. 2023, doi: 10.3390/en16031244.

[7] B. V. Rajanna and M. K. Kumar, "Comparison study of lead-acid and lithium-ion batteries for solar photovoltaic applications," *International Journal of Power Electronics and Drive Systems (IJPEDS)*, vol. 12, no. 2, p. 1069, Jun. 2021, doi: 10.11591/ijpeds.v12.i2.pp1069-1082.

[8] H. Keshan, J. Thornburg, and T. S. Ustun, "Comparison of lead-acid and lithium ion batteries for stationary storage in off-grid energy systems," in *4th IET Clean Energy and Technology Conference (CEAT 2016)*, Institution of Engineering and Technology, 2016, pp. 30 (7 .)-30 (7 .), doi: 10.1049/cp.2016.1287.

[9] M. Banerjee and H. Kaur, "A Comparison Among Lithium-Ion, Nickel-Cadmium amp; Nickel-Metal-Hydride Batteries for Charging and Discharging in Electric Vehicle by Bidirectional DC-DC Converter," in *2022 IEEE IAS Global Conference on Emerging Technologies (GlobConET)*, IEEE, May 2022, pp. 361–368, doi: 10.1109/GlobConET53749.2022.9872335.

[10] M. B. Sanjareh, M. H. Nazari, M. Ebadat-Parast, and S. H. Hosseinian, "Cost comparison of various battery technologies for hybrid energy storage system application in an islanded Microgrid," in *2021 11th Smart Grid Conference (SGC)*, IEEE, Dec. 2021, pp. 1–6, doi: 10.1109/SGC54087.2021.9664077.

[11] S. Nagaraju and N. K. Ramaswamy, "Decentralized dynamic power control in an islanded DC microgrid with hybrid energy storage system," *International Journal of Power Electronics and Drive Systems (IJPEDS)*, vol. 13, no. 4, p. 2190, Dec. 2022, doi: 10.11591/ijpeds.v13.i4.pp2190-2198.

[12] X. Lin and R. Zamora, "Controls of hybrid energy storage systems in microgrids: Critical review, case study and future trends," *Journal of Energy Storage*, vol. 47, p. 103884, Mar. 2022, doi: 10.1016/j.est.2021.103884.

[13] S. M. Mousavi, S. H. Fathi, and G. H. Riahy, "Energy management of wind/PV and battery hybrid system with consideration of memory effect in battery," in *2009 International Conference on Clean Electrical Power*, IEEE, Jun. 2009, pp. 630–633, doi: 10.1109/ICCEP.2009.5211989.

[14] N. M. L. Tan, T. Abe, and H. Akagi, "Design and Performance of a Bidirectional Isolated DC–DC Converter for a Battery Energy Storage System," *IEEE Transactions on Power Electronics*, vol. 27, no. 3, pp. 1237–1248, Mar. 2012, doi: 10.1109/TPEL.2011.2108317.

[15] M. P. Akter, S. Mekhilef, N. M. L. Tan, and H. Akagi, "Model Predictive Control of Bidirectional AC-DC Converter for Energy Storage System," *Journal of Electrical Engineering and Technology*, vol. 10, no. 1, pp. 165–175, Jan. 2015, doi: 10.5370/JEET.2015.10.1.165.

[16] A. Subramanian and S. KR, "Review of multiport isolated bidirectional converter interfacing renewable and energy storage system," *International Journal of Power Electronics and Drive Systems (IJPEDS)*, vol. 11, no. 1, p. 466, Mar. 2020, doi: 10.11591/ijpeds.v11.i1.pp466-467.

[17] K. Bathala, D. Kishan, and N. Harischandrappa, "High frequency isolated bidirectional dual active bridge DC-DC converters and its application to distributed energy systems: an overview," *International Journal of Power Electronics and Drive Systems (IJPEDS)*, vol. 14, no. 2, p. 969, Jun. 2023, doi: 10.11591/ijpeds.v14.i2.pp969-991.

[18] G. Ranipriya, R. Jegatheesan, and K. Vijayakumar, "Partially isolated four port converter with combined PWM and secondary phase shift control," *International Journal of Electrical and Computer Engineering (IJECE)*, vol. 11, no. 2, p. 1086, Apr. 2021, doi: 10.11591/ijece.v11i2.pp1086-1094.

[19] A. Andang, R. S. Hartati, I. B. G. Manuaba, and I. N. S. Kumara, "Three-phase four-wire shunt hybrid active power filter model with model predictive control in imbalance distribution networks," *International Journal of Electrical and Computer Engineering (IJECE)*, vol. 12, no. 6, p. 5923, Dec. 2022, doi: 10.11591/ijece.v12i6.pp5923-5937.

[20] F. Rojas *et al.*, "An Overview of Four-Leg Converters: Topologies, Modulations, Control and Applications," *IEEE Access*, vol. 10, pp. 61277–61325, 2022, doi: 10.1109/ACCESS.2022.3180746.

[21] E. Ayoubi, M. R. Miveh, A. A. Ghadimi, and S. Bagheri, "Enhanced controller for a four-leg inverter operating in a stand-alone microgrid with unbalanced loads," *International Journal of Power Electronics and Drive Systems (IJPEDS)*, vol. 12, no. 4, p. 2372, Dec. 2021, doi: 10.11591/ijpeds.v12.i4.pp2372-2383.

[22]   N. A. Ninad and L. Lopes, "Per-phase vector control strategy for a four-leg voltage source inverter operating with highly unbalanced loads in stand-alone hybrid systems," *International Journal of Electrical Power & Energy Systems*, vol. 55, pp. 449–459, Feb. 2014, doi: 10.1016/j.ijepes.2013.09.019.

[23]   M. J. H. Moghaddam *et al.*, "Improved Voltage Unbalance and Harmonics Compensation Control Strategy for an Isolated Microgrid," *Energies*, vol. 11, no. 10, p. 2688, Oct. 2018, doi: 10.3390/en11102688.

[24]   X. Chen, Z. Wei, H. Wang, C. Li, and C. Gong, "Research of three-phase four-leg rectifier," in *IECON 2012 - 38th Annual Conference on IEEE Industrial Electronics Society*, IEEE, Oct. 2012, pp. 719–724, doi: 10.1109/IECON.2012.6388663.

[25]   R. Zhang, F. C. Lee, and D. Boroyevich, "Four-legged three-phase PFC rectifier with fault tolerant capability," in *2000 IEEE 31st Annual Power Electronics Specialists Conference. Conference Proceedings (Cat. No.00CH37018)*, IEEE, pp. 359–364, doi: 10.1109/PESC.2000.878878.

[26]   M. P. Kazmierkowski, M. A. Dzieniakowski, and W. Sulkowski, "The three phase current controlled transistor DC link PWM converter for bi-directional power flow," in *in Proc. PEMC Conf.*, 1990, pp. 465–469,

[27]   T. Ohnishi, "Three phase PWM converter/inverter by means of instantaneous active and reactive power control," in *Proceedings IECON '91: 1991 International Conference on Industrial Electronics, Control and Instrumentation*, IEEE, 1991, pp. 819–824, doi: 10.1109/IECON.1991.239183.

[28]   A. Mohamed, A. Nejadpak, and O. Mohammed, "LCL-filter-based bi-directional converter for connectivity of microgrids involving sustainable energy sources," in *2012 North American Power Symposium (NAPS)*, IEEE, Sep. 2012, pp. 1–6, doi: 10.1109/NAPS.2012.6336334.

[29]   D. Cittanti, F. Mandrile, M. Gregorio, and R. Bojoi, "Design Space Optimization of a Three-Phase LCL Filter for Electric Vehicle Ultra-Fast Battery Charging," *Energies*, vol. 14, no. 5, p. 1303, Feb. 2021, doi: 10.3390/en14051303.

[30]   N. Mdini, S. Skander-Mustapha, and I. Slama-Belkhodja, "Design of passive power filters for battery energy storage system in grid connected and islanded modes," *SN Applied Sciences*, vol. 2, no. 5, p. 933, May 2020, doi: 10.1007/s42452-020-2747-7.

[31]   X. Li, Z. Deng, Z. Chen, and Q. Fei, "Analysis and Simplification of Three-Dimensional Space Vector PWM for Three-Phase Four-Leg Inverters," *IEEE Transactions on Industrial Electronics*, vol. 58, no. 2, pp. 450–464, Feb. 2011, doi: 10.1109/TIE.2010.2046610.

[32]   A. S. Abdulsada, I. M. Abdulbaqi, and A. H. Ahmed, "A study of feeding an unbalanced load from a four-leg 3-phase inverter using SVPWM technique," in *2018 1st International Scientific Conference of Engineering Sciences - 3rd Scientific Conference of Engineering Science (ISCES)*, IEEE, Jan. 2018, pp. 215–220, doi: 10.1109/ISCES.2018.8340556.

[33]   I. M. Abdulbaqi, A. H. Ahmed, and A. S. Abdulsada, "A Study of a 3-Phase Four-Leg Inverter Dynamic Operation," in *2018 International Conference on Engineering Technology and their Applications (IICETA)*, IEEE, May 2018, pp. 66–71, doi: 10.1109/IICETA.2018.8458095.

[34]   I. M. Abdulbaqi, A. H. Ahmed, R. G. Omar, and A. S. Abdulsada, "Modeling and Analysis of a Four-Leg Inverter Using Space Vector Pulse Width Modulation Technique," *Journal of Engineering and Sustainable Development*, vol. 23, no. 2, pp. 100–119, Feb. 2019, doi: 10.31272/jeasd.23.2.9.

[35]   R. Zhang, V. H. Prasad, D. Boroyevich, and F. C. Lee, "Three-dimensional space vector modulation for four-leg voltage-source converters," *IEEE Transactions on Power Electronics*, vol. 17, no. 3, pp. 314–326, May 2002, doi: 10.1109/TPEL.2002.1004239.

[36]   A. Özdemir and Z. Erdem, "Optimal digital control of a three-phase four-leg voltage source inverter," *Turkish Journal Of Electrical Engineering & Computer Sciences*, vol. 24, pp. 2220–2238, 2016, doi: 10.3906/elk-1310-102.

[37]   M. P. Kazmierkowski, R. Krishnan, and F. Blaabjerg, *Control in Power Electronics: Selected Problems*. Academic Press An imprint of Elsevier Science, 2003. doi: 10.1016/B978-0-12-402772-5.X5000-5.

BIOGRAPHIES OF AUTHORS

Nikita A. Dobroskok 🆔 ⑧ ⓈⒸ ◗ is an associate professor in Saint-Petersburg electrotechnical university "LETI", Saint-Petersburg, Russia. In 2012, he received a master's degree in engineering and technology in the direction of automation and control at the Saint-Petersburg electrotechnical university. In 2014, he received a Ph.D. degree in technical sciences with a degree in Electrical Complexes and Systems (Saint-Petersburg electrotechnical university). Until 2020, he worked at the Central Research Institute of Marine Electrical Engineering and Technology branch of State Krylov Research Center. Since 2016, he has held the position of an associate professor of the Department of Automatic Control Systems, LETI. Field of work: theory of automatic control, electric drive. He is the author of over 40 publications. Research interests: AC varied frequency drives; static frequency converters. He can be contacted at email: nadobroskok@etu.ru.

Anastasiia D. Stotckaia 🆔 ⑧ ⓈⒸ ◗ was born in Leningrad (Russia) 01/01/1987. In 2010 graduated from the Saint-Petersburg Electrotechnical University "LETI" with master degree in control and automation of industrial mechatronic systems and special moving objects. In 2013 Anastasiia D. Stotckaia defended thesis and received a Ph.D. degree in the specialty "Electrotechnical complexes and systems" (Saint-Petersburg Electrotechnical University "LETI", Saint-Petersburg, Russia). Since 2014, she has been working as an assistant professor at the Department of Automatic Control Systems, since 2022 she has been the dean of the Faculty of Electrical Engineering and Industrial Automation. Major field of study - automatic control, modern control methods, electrical engineering. She is an author of over 40 publications and has 10 certificates of registration of software tools. Current research interests: high-speed rotation machinery, mathematical modeling, and nonlinear systems. She can be contacted at email: adstotckaia@etu.ru.

Ruslan M. Migranov 🆔 Ⓖ SC ↻ was born in Tashkent, Uzbekistan on 03/04/1999. In 2021, he graduated from the Saint-Petersburg Electrotechnical University "LETI" with a barchelor's and master degrees in Department of Automatic Control Systems, where since 2021 he has been worked as engineer and continue his education in Ph.D. He can be contacted at email: rmmigranov@etu.ru.

Victor S. Lavrinovskiy 🆔 Ⓖ SC ↻ is an assistant in Saint-Petersburg electrotechnical university "LETI", Saint-Petersburg, Russia. He received his B.Eng., M.Eng. degrees in Saint-Petersburg electrotechnical university "LETI", in 2010 and 2012, respectively. His research interests include the field of modular converters, hybrid propulsion systems and power electronics. He can be contacted at email: vslavrinovskii@etu.ru.

Perevalov Yurii Yurievich 🆔 Ⓖ SC ↻ is an associate professor at the department of ETPT at the St. Petersburg State Electrotechnical University "LETI". Since 2021 he has been a member of the Scientific and Technical Committee of St. Petersburg Electrotechnical University "LETI", since 2022 he has been a member of the Council of the FEA of St. Petersburg State Technical University "LETI". Since 2009, he has been working part-time at INTERM Corporation, currently holding the position of senior researcher. The main scientific interests at the moment are Complex multiphysics mathematical models of induction heat treatment of mechanical engineering products, with the calculation of electromagnetic, temperature fields, voltage fields, taking into account the characteristics of power supplies and matching devices. He can be contacted at email: yyperevalov@yandex.ru.

Artem S. Melnikov 🆔 Ⓖ SC ↻ is an assistant at the St. Petersburg Electrotechnical University "LETI", St. Petersburg, Russia. In 2021, he received a master's degree in Engineering and Technology in the direction of "Electric power and electrical engineering" at St. Petersburg Electrotechnical University. Since 2021, he has been studying at the postgraduate school of ETU "LETI". He is the author of 15 publications and 2 patents. His research interests are magnetic pulse metal processing and power electronics. He can be contacted at email: asmelnikov@etu.ru.

Vyacheslav Parmenov 🆔 Ⓖ SC ↻ is a postgraduate student and engineer in Saint Petersburg Electrotechnical University "LETI". He received his Bachelor's and Master's degrees in Department of Electrical Technology and Converter Engineering in 2019 and 2021 respectively. During his studies and work, he wrote 7 publications, was the executor of 8 research projects, and also participated in the writing of 2 patents, one of which was on the topic "Magnetic pulse installation for assembly operations". He proposed and implemented the idea of using a digital control system for charging and discharging high-voltage capacitor banks. His research interests include the control systems digitalization and the digital twin's introduction in induction heating technology. He can be contacted at email: veparmenov@etu.ru.

Nazar V. Maslennikov 🆔 Ⓖ SC ↻ is a graduate of the Master's degree in 2023 of the Department of Electrical Technology and Converter Engineering of the Saint Petersburg Electrotechnical University "LETI", St. Petersburg, Russia. Currently, he continues to work as an engineer. During his time as an engineer, he wrote 5 publications, won two grants and was the executor of 4 R&D projects, and also participated in writing patents, one of which was written on the topic of "Applying protective coatings by thermodiffusion method", proposing and implementing the idea of using high-frequency power sources. Currently, there is a large reserve on this topic for the development of the developed technology. He can be contacted at email: nvmaslennikov@etu.ru.